



## OPEN ACCESS

## EDITED BY

Siamak Hoseinzadeh,  
Sapienza University of Rome, Italy

## REVIEWED BY

Hassan Bazazzadeh,  
Poznań University of Technology, Poland  
Masoud Norouzi,  
University of Rovira i Virgili, Spain  
Farbod Esmailion,  
K. N. Toosi University of Technology, Iran

## \*CORRESPONDENCE

Xiuyun Wang,  
✉ w-xiu-y@163.com

RECEIVED 15 April 2023

ACCEPTED 22 June 2023

PUBLISHED 12 July 2023

## CITATION

Wang R, Wen X, Wang X, Fu Y and Zhao Y (2023), Low-carbon economic dispatch of regional integrated energy system based on carbon-oxygen cycle. *Front. Energy Res.* 11:1206242. doi: 10.3389/fenrg.2023.1206242

## COPYRIGHT

© 2023 Wang, Wen, Wang, Fu and Zhao. This is an open-access article distributed under the terms of the [Creative Commons Attribution License \(CC BY\)](https://creativecommons.org/licenses/by/4.0/). The use, distribution or reproduction in other forums is permitted, provided the original author(s) and the copyright owner(s) are credited and that the original publication in this journal is cited, in accordance with accepted academic practice. No use, distribution or reproduction is permitted which does not comply with these terms.

# Low-carbon economic dispatch of regional integrated energy system based on carbon-oxygen cycle

Rutian Wang<sup>1</sup>, Xiangyun Wen<sup>1</sup>, Xiuyun Wang<sup>1\*</sup>, Yanbo Fu<sup>2</sup> and Yanfeng Zhao<sup>3</sup>

<sup>1</sup>Key Laboratory of Modern Power System Simulation and Control & Renewable Energy Technology, Ministry of Education (Northeast Electric Power University), Jilin, China, <sup>2</sup>School of Electrical Engineering, Yanshan University, Qinhuangdao, China, <sup>3</sup>State Grid Jibei Electric Power Company, Chengde Power Supply Company, Chengde, China

In order to solve the contradiction between energy supply and carbon emissions, using P2G to combine oxy-fuel combustion power plant with gas turbines. According to the laws of mass conservation and energy conservation, carbon and oxygen elements are introduced into the model in the form of gases to construct an energy hub model for the carbon oxygen cycle system. To solve the problem of time imbalance between interconnected devices, a flexible operation mode using storage devices as connection hubs is proposed. Based on the constraints of the system's operating mechanism, study the variation range of the operating range and establish an objective function with the optimal operating cost. Optimize the operation of the combined system, study the change interval of its operation range, and analyze the scheduling model under three different operation models. Low-Carbon economic model of combined system is established in regional integrated energy system. The results show that the basic carbon oxygen cycle model can save 9.14% economic cost and reduce 44.05% carbon emission. The carbon oxygen cycle capacity increasing mode can save 13.05% economic cost and reduce 59.91% carbon emission. Carbon and oxygen circulation system in improving renewable energy consumption and reducing carbon dioxide emissions is verified by an example.

## KEYWORDS

oxy-fuel combustion, carbon-oxygen flow, power to gas, carbon emissions, regional integrated energy system

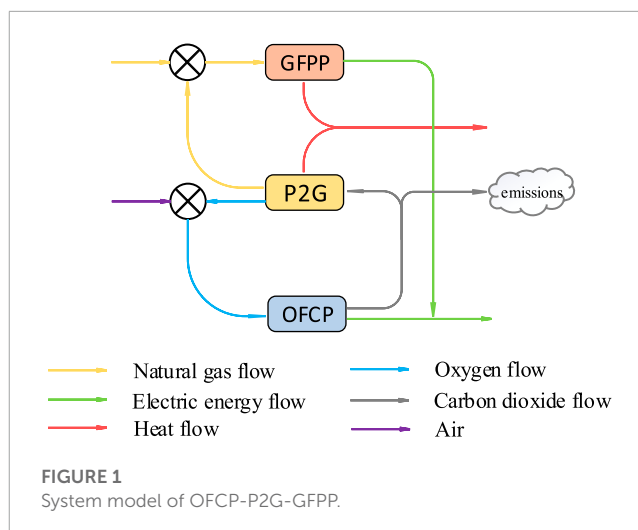
## 1 Introduction

Environmental pollution, climate warming and fossil energy crisis all over the world pose a serious threat to sustainable development. At the 21st United Nations Climate Change Conference, many countries signed the Paris Agreement. In response to the international call, governments of various countries have made their own low-carbon commitments (UNCC, 2016). China announced at the 75th session of the UN General Assembly that it would enhance national independent contribution. It will strive to reach the peak of carbon dioxide emissions by 2030 and achieve carbon neutrality by 2060. Electricity production is one of the main sources of greenhouse gas emissions, which is facing huge pressure to reduce carbon emissions. Integrated energy system has obvious potential for Low-Carbon

emission reduction, which integrates and optimizes electricity, gas, heat and other energy sources (Wang et al., 2020; Hua et al., 2020). Integrated energy system integrates electricity, gas and heat, and forms the integration of energy production, supply and marketing, which has become a research hotspot in the field of international energy (Gu et al., 2017; Wang et al., 2019).

Energy crisis and other issues have accelerated the application and promotion of regional integrated energy systems (RIES). RIES research is more suitable for China's national conditions. The region is generally recognized as a region, a city, a town, etc. The concept of energy Internet (EI) is proposed (Dong and Zhao, 2014), which is conducive to the adjustment of energy structure and provides a new way to solve the problem of the acceptance of renewable energy. However, wind power generation has strong random volatility and typical anti-peak shaving characteristics, which has an adverse effect on the consumption of renewable energy (Lu et al., 2019). In 2010, the Fraunhofer Research Center in Germany put forward the concept of "electricity to gas" for the first time, which is expected to solve the problems of wind abandonment and energy storage (Energy Resource Guide, 2010). In 2003, the Swiss Federal Institute of Technology Zurich carried out research on energy planning projects (Favre-Perrod, 2005), analyzing the complementary advantages of multiple energy systems from various angles. And the idea of energy hub (EH) was first proposed in the literature (Geidl, 2007). In literature (Wang et al., 2017), an electric gas coupling link with EH as the core is constructed to study the interaction between electric power and natural gas system. Literature (Zhang, 2015) proposes an EH model with multiple energy systems, which represents the coupling between various energy infrastructures. It is used to supply electric power, natural gas and thermal loads. But in the above research, EH is only limited to the coupling of electricity, gas and thermal energy. The model of input and output transmitted in the form of gas energy flow is not considered and the source and recovery of gas are ignored. There are problems such as extra investment and energy loss.

In order to reduce the intensity of carbon emissions and alleviate climate change, carbon capture and encapsulation technology is an effective way, which has received extensive attention worldwide. Literatures (Viebahn et al., 2015; Viebahn et al., 2014) evaluate the feasibility of carbon capture and storage technologies in India and China respectively. Carbon capture technology mainly includes post-combustion capture technology, pre-combustion capture technology and oxy-fuel combustion technology. Among them, oxy-fuel combustion technology has many advantages and has become one of the technologies with great prospects (Ghorbani et al., 2018). The research on carbon capture technology is increasing, and the utilization of carbon dioxide has become a hot research field. Literature (Viklund and Karlsson, 2015) analyzes the relationship between waste heat used in energy system and carbon dioxide emissions. Literature (Karjunen et al., 2017) evaluates different implementation strategies of CO<sub>2</sub> utilization system. Literature (Zhou et al., 2018) proposes power to gas (P2G) and carbon capture power plants as a unified system, carbon capture power plants provide raw material CO<sub>2</sub> for P2G, and establishes a coordinated optimization model. Literature (Yang, 2019) proposes the concept of a combined system of P2G and gas turbine, which converts CO<sub>2</sub> into gas-fired power plant (GFPP) fuel, and establishes



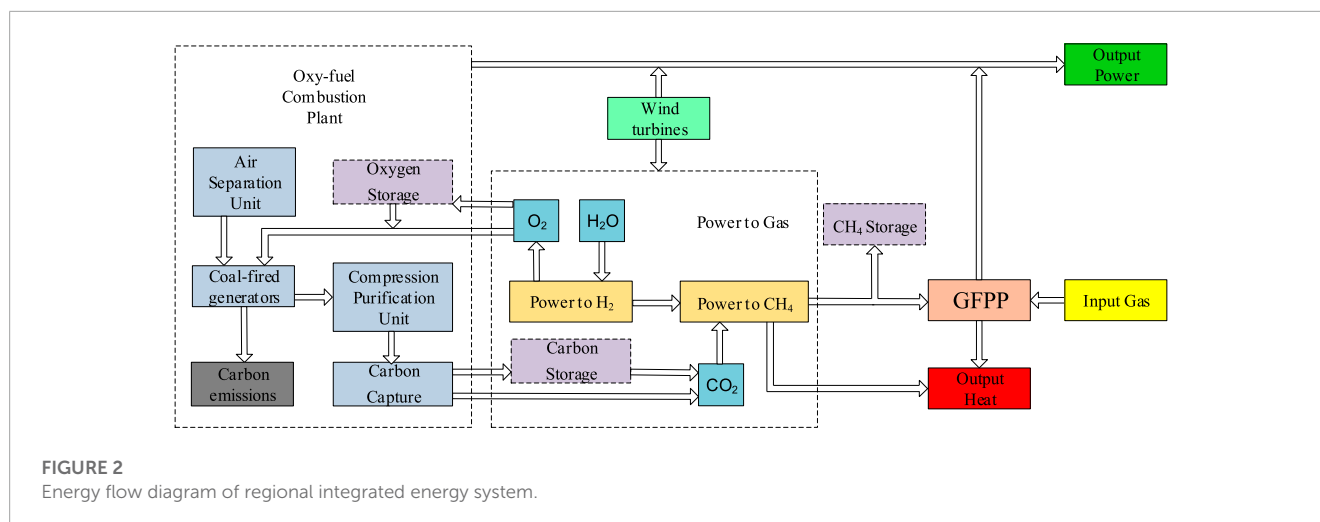
a model of the GFPP-P2G combined system. Literature (Cui et al., 2020) proposes to introduce oxy-fuel combustion technology into the electricity-gas-heat RIES, and establishes a low-carbon model of P2G and oxy-fuel combustion plant (OFCP). The above research proves that the combined model can better improve the level of carbon utilization. However, the utilization of O<sub>2</sub> in P2G technology and the incomplete absorption of OFCP are not considered, which causes time imbalance between systems, and further research is needed.

In response to the above problems, this article considers the gas energy flow, gas source and recovery problems in the traditional EH. An innovative energy cycle model for oxy-fuel combustion and power to gas is proposed, avoiding unnecessary energy loss and additional investment. And a new mathematical model of combined system is established from the point of view of amount of substance. To solve the problem of unequal time between interconnected devices, the flexible operation mode with storage devices as the connection hub is proposed. In Section 2, the interconnection of OFCP and P2G forms an energy circulation. In Section 3, construct the EH model of the OFCP-P2G-GFPP combination system, and introduce carbon and oxygen into the model in the form of gas. In Section 4, the power gas regional integrated energy system scheduling model based on the interconnection of P2G and OFCP is established. In Section 5, an example is given to verify the low-carbon and economic performance of the proposed model. In Section 6, draw the conclusion.

## 2 Model of OFCP-P2G-GFPP

At present, the carbon emission of power industry mainly comes from coal-fired power plants, which leads to the contradiction between energy supply and carbon emission. This article mainly conducts related research on reducing carbon emissions in terms of transformation technology. Use P2G technology to combine OFCP with GFPP. The basic idea of joint operation of OFCP-P2G-GFPP system is shown in Figure 1.

P2G technology uses electric energy to hydrolyze to produce H<sub>2</sub> and O<sub>2</sub>. H<sub>2</sub> reacts with CO<sub>2</sub> to generate CH<sub>4</sub>, which is transported



to GFPP through natural gas pipeline.  $O_2$  is transmitted to OFCP, and high-concentration  $O_2$  is used instead of air to achieve the purpose of combustion and obtain high purity  $CO_2$  stream. After further compression and purification,  $CO_2$  can be captured and stored, and returned to the P2G equipment as a raw material. The output power of GFPP and OFCP supplies power for the power load. The heat released in the process of  $CH_4$  generation and the high temperature flue gas discharged by GFPP can provide heat energy for the thermal load. Thus, energy can be locked in the annular OFCP-P2G-GFPP combined system to achieve energy recycling. It can not only effectively reduce  $CO_2$  emissions, but also reduce the operating cost of the system, which can realize low-carbon power generation.

In RIES, the thermal power units are transformed into low-carbon units. OFCP is mainly composed of air separation unit (ASU), compression purification unit (CPU) and oxygen-enriched boilers. The energy consumption of ASU and CPU is provided by thermal power plant. The conversion energy consumption of P2G is provided by renewable energy, which provides an effective way for wind energy consumption. The specific energy flow relationship among units is shown in Figure 2.

P2G technology can improve the capacity of wind power absorption and provide a new way for the use of renewable energy. It converts the remaining wind energy into natural gas, which is transmitted to GFPP for the production of electric energy and heat energy. In order to solve the problem of time imbalance between P2G and GFPP, gas storage equipment can be added. And the temporary surplus natural gas will be collected into the gas storage equipment for storage. P2G recycles  $CO_2$  captured by OFCP, but only when there is abandoned air in the system, can P2G start to produce  $CH_4$ . While OFCP always produces by-product  $CO_2$  during operation. In order to solve the problem of time inequality between the two, carbon storage equipment will be added to the system, which can save the cost of  $CO_2$  packaging and the raw material cost of P2G purchasing high-purity  $CO_2$ . On the other hand, ASU realizes the separation of oxygen from air and supplies it to thermal power units. If ASU produces too much oxygen, it can only increase the output of the thermal power unit, that is to say, the power supply is determined by oxygen. In order to avoid

this phenomenon, the  $O_2$  produced by P2G is liquefied under the action of cryogenic pump and transported to the liquid oxygen tank of OFCP for storage. When using  $O_2$ , a vaporizer can be used to volatilize liquid oxygen into gas. The increase of energy storage equipment can effectively reduce the operation cost and unnecessary energy loss of the system. And the economic benefits and low-carbon operation have been improved, reflecting the advantages of multi-energy system interconnection.

## 3 Low-carbon model of OFCP-P2G-GFPP

### 3.1 Basic model of OFCP-P2G-GFPP

EH is used as coupling element in RIES. Considering the energy source and Low-Carbon emission of P2G, a new EH model is established, and the transfer form of gas energy flow is introduced into the EH model. The new EH is embodied in the basic model of the OFCP-P2G-GFPP system, as shown in Figure 3.

According to the law of conservation of mass and the law of conservation of energy, the OFCP-P2G-GFPP combined system model can be established. Among them, the variables  $P$  and  $H$  are the electric energy and heat energy transmitted by the system, and the unit is  $MW$ .  $W$  stands for renewable energy,  $n$  stands for the number of substances in each gas medium, the unit is  $mol$ . In the parameter subscript,  $i$  and  $o$  are the input and output of the combined system,  $c$  is the variable internally converted by the EH,  $p$  is the energy produced by each unit and equipment, and the parameter is the gas type.

According to the law of conservation of mass, in OFCP and P2G equipment, the sum of the total amount of substances before reaction is equal to the sum of the amount of substances after reaction. Thermal power plant is the core part of OFCP. The amount of coal used for combustion  $n_i^C$ , the amount of oxygen generated by the P2G equipment  $n_c^{O_2}$ , and the amount of oxygen generated by ASU  $n_p^{O_2}$  are combined into the combustion chamber. However, in the operation process of thermal power units, part of  $CO_2$  is trapped and packaged, and the amount of carbon element recovery and

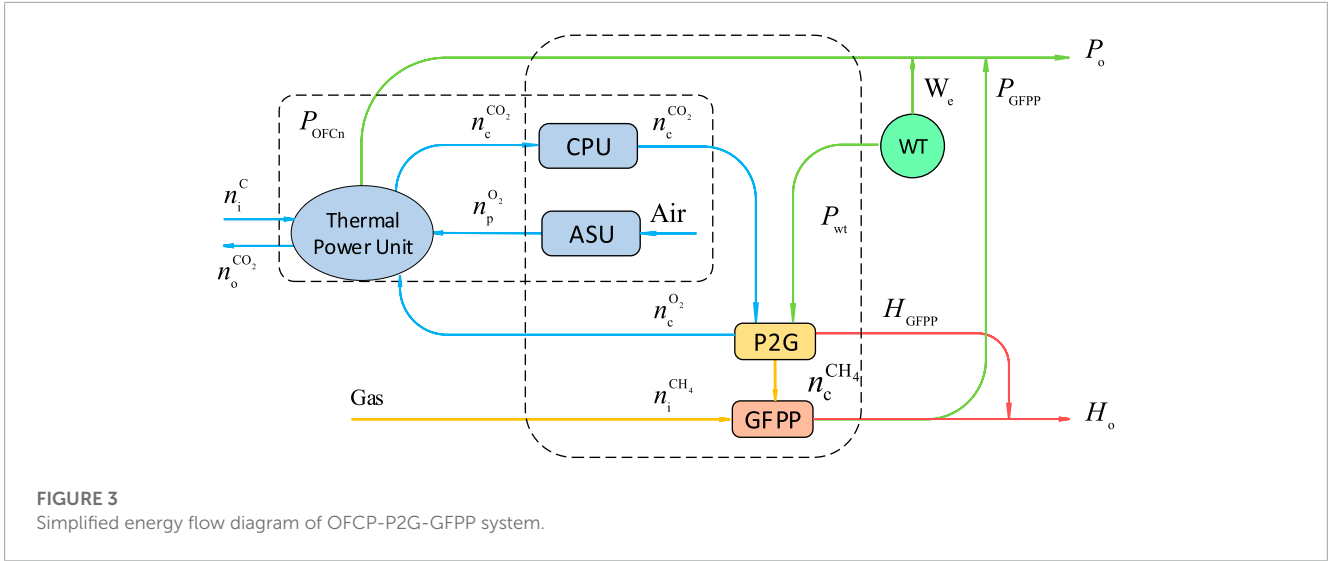
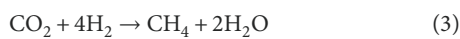


**FIGURE 3**  
Simplified energy flow diagram of OFCP-P2G-GFPP system.

utilization is  $n_c^{CO_2}$ . There is also the remaining unused carbon dioxide  $n_o^{CO_2}$  being emitted. From this, we can get the law of conservation of mass in OFCP stage, as shown in Eq. 1. P2G converts electrical energy into natural gas energy, where the reactants are water used for electrolysis  $n_c^{H_2O}$  and  $n_c^{CO_2}$ , generating output in the form of  $CH_4$   $n_c^{CH_4}$  and  $n_c^{O_2}$ .

$$n_i^C + (n_c^{O_2} + n_p^{O_2}) = n_c^{CO_2} + n_o^{CO_2} \quad (1)$$

The chemical equations of the two reaction stages of P2G are shown in Eqs 2, 3. Under standard conditions, the stoichiometric number in the P2G total reaction equation can also reflect the relationship between the amounts of each gaseous substance, as shown in Eq. 4.



$$n_c^{CH_4} = n_c^{CO_2} = \frac{1}{2}n_c^{O_2} = \frac{1}{4}n_c^{H_2} \quad (4)$$

According to the simplified energy flow diagram of OFCP-P2G-GFPP system, it can be known from the law of conservation of energy that the main output of the OFCP system is the thermal power unit. The output electric energy of the unit is  $P_Z$ , the energy produced by OFCP in a unit oxygen environment is  $\epsilon^{O_2}$ , and Eq. 5 represents the output of the thermal power unit. The energy consumption of the OFCP system can be divided into two parts: basic energy consumption and operating energy consumption. The basic energy consumption has nothing to do with the operating state of the OFCP, which can be regarded as constant. Operating energy consumption is mainly the energy loss produced by the oxy-fuel combustion system in the process of air separation, capture and compression. It is related to the operating state of OFCP, that is, energy consumption is air separation energy consumption  $P_{ASU}$  and compression purification energy consumption  $P_{CPU}$ . As shown in Eqs 6 and 7,  $\eta_{ASU}^{O_2}$  and  $\eta_{CPU}^{CO_2}$  represents the conversion efficiency of the air separation unit and the carbon capture unit;  $\lambda_g^{O_2}$  and  $\lambda_g^{CO_2}$

represents the electric energy consumed by manufacturing unit  $O_2$  and capturing unit  $CO_2$ .

$$P_Z = \epsilon^{O_2}(n_c^{O_2} + n_p^{O_2}) \quad (5)$$

$$P_{ASU}\eta_{ASU}^{O_2} = \lambda_g^{O_2}n_p^{O_2} \quad (6)$$

$$P_{CPU}\eta_{CPU}^{CO_2} = \lambda_g^{CO_2}n_c^{CO_2} \quad (7)$$

Since P2G is a highly exothermic reaction, the heat generated by it can be transferred to the heating system. The heat value generated by the reaction per mole of  $CH_4$  is  $\phi_{te}$ , and the heat energy generated in the total reaction stage is  $H_{P2G}$ , as shown in Eq. 8. P2G converts the remaining wind power into natural gas through electrolysis, as shown in Eq. 9.  $P_{WT}$  represents the output value of wind turbine,  $\phi^{H_2}$  represents the wind energy consumed by converting P2G into  $H_2$  per mole, and  $\eta_{P2G}^{H_2}$  represents the efficiency of wind turbine.

$$H_{P2G} = \phi_{te}n_c^{CH_4} \quad (8)$$

$$P_{WT}\eta_{P2G}^{H_2} = \phi^{H_2}n_c^{H_2} \quad (9)$$

Natural gas and P2G jointly provide energy for GFPP unit, and the unit performs work to convert natural gas into energy for utilization.  $P_{GFPP}$  and  $H_{GFPP}$  are the electricity and heat output by GFPP, and  $\eta_e^{CH_4}$ ,  $\eta_h^{CH_4}$  are the conversion efficiency of GFPP from natural gas to electricity and heat, as shown in Eqs 10, 11.

$$P_{GFPP} = \eta_e^{CH_4}\phi^{CH_4}(n_c^{CH_4} + n_i^{CH_4}) \quad (10)$$

$$H_{GFPP} = \eta_h^{CH_4}\phi^{CH_4}(n_c^{CH_4} + n_i^{CH_4}) \quad (11)$$

In the basic operation mode of the combined system, the law of conservation of mass is used to calculate  $CO_2$  emissions, as shown in Eq. 12.

$$\begin{aligned} n_{o1}^{CO_2} &= n_i^C + (n_c^{O_2} + n_p^{O_2}) - n_c^{CO_2} \\ &= n_i^C + n_p^{O_2} + n_c^{CO_2} \\ &= n_i^C + \frac{n_g^{O_2}}{\lambda_g^{O_2}}P_{ASU} + \frac{n_g^{CO_2}}{\lambda_g^{CO_2}}P_{CPU} \end{aligned} \quad (12)$$

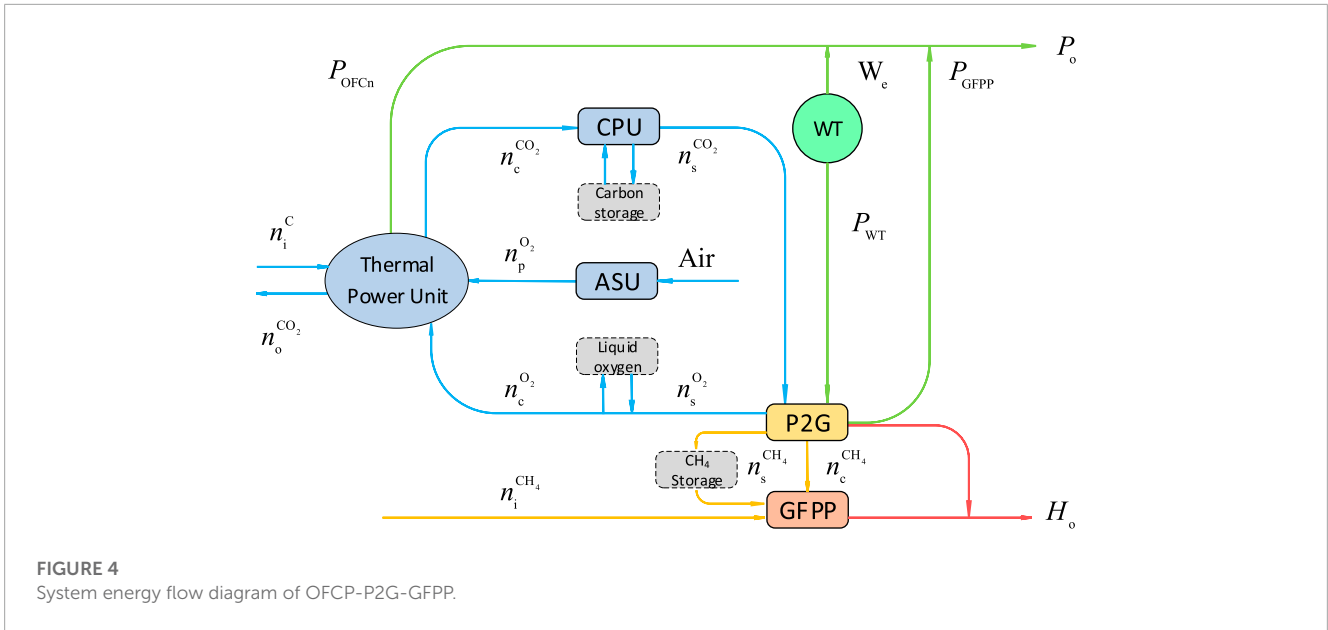


FIGURE 4 System energy flow diagram of OFCP-P2G-GFPP.

The output power of the basic operation mode  $P_{o1}$  is the sum of the net output power of OFCP  $P_{OFcPn1}$  and the output power of GFPP unit  $P_{GFPP}$ . And the output energy  $P_Z$  of the thermal power unit is used to subtract the energy loss of the ASU and CPU equipment to obtain  $P_{OFcPn1}$ . Then solve and sum the basic output electric energy can get that the basic output electric energy is composed of the energy generated by the independent operation of OFCP  $P_{OFcP}$ , the energy transmitted by external natural gas source and the energy of renewable energy, which is shown in Eq. 13.

$$\begin{aligned}
 P_{o1} &= P_{OFcPn1} + P_{GFPP} \\
 &= \varepsilon_{O_2} (n_c^{O_2} + n_p^{O_2}) - \frac{\lambda_g^{O_2} n_p^{O_2}}{\eta_{ASU}} - \frac{\lambda_g^{CO_2} n_c^{CO_2}}{\eta_{CPU}} \\
 &\quad + \eta_e^{CH_4} \varphi^{CH_4} (n_c^{CH_4} + n_i^{CH_4}) \\
 &= \left[ \left( \varepsilon_{O_2} - \frac{\lambda_g^{O_2}}{\eta_{ASU}} \right) n_p^{O_2} - \frac{\lambda_g^{CO_2} n_c^{CO_2}}{\eta_{CPU}} \right] + \eta_e^{CH_4} \varphi^{CH_4} n_i^{CH_4} \quad (13) \\
 &\quad + \frac{(2\varepsilon_{O_2} + \eta_e^{CH_4} \varphi^{CH_4}) \eta_{P2G}^{H_2}}{4\varphi^{H_2}} P_{WT} \\
 &= P_{OFcP} + \eta_e^{CH_4} E_i + \eta^e P_{WT}
 \end{aligned}$$

Among them,  $E_i$  is the energy converted from the natural gas network to the GFPP equipment,  $\eta^e$  is the equivalent conversion efficiency of the remaining renewable energy wind energy into electrical energy. In the OFCP-P2G-GFPP system,  $\eta^e P_{WT}$  is the unique increase in energy of the combined system. Part of the energy is used for  $CO_2$  capture and  $O_2$  exchange, and the rest is used for load supply.

The output heat of the basic operation model  $H_{o1}$  is the sum of the heat released by the P2G  $H_{P2G}$  and the heat output of the GFPP unit  $H_{GFPP}$ . Part of the output heat energy of GFPP and the heat energy released by P2G depend on the connection of the OFCP-P2G-GFPP combined system, which can absorb the remaining

renewable energy. Another part of GFPP output heat energy comes from natural gas network transmission energy, as shown by Eq. 14.

$$\begin{aligned}
 H_{o1} &= H_{P2G} + H_{GFPP} \\
 &= \varphi_{te} n_c^{CH_4} + \eta_h^{CH_4} \varphi^{CH_4} (n_c^{CH_4} + n_i^{CH_4}) \\
 &= \eta_h^{CH_4} \varphi^{CH_4} n_i^{CH_4} + (\varphi_{te} + \eta_h^{CH_4} \varphi^{CH_4}) n_c^{CH_4} \quad (14) \\
 &= \eta_h^{CH_4} E_i + \frac{(\varphi_{te} + \eta_h^{CH_4} \varphi^{CH_4}) \eta_{P2G}^{H_2}}{4\varphi^{H_2}} P_{WT} \\
 &= \eta_h^{CH_4} E_i + \eta^h P_{WT}
 \end{aligned}$$

$\eta^e$  is the equivalent conversion efficiency of abandoned wind into electric energy. In the OFCP-P2G-GFPP system,  $\eta^h P_{WT}$  is the unique increase in heat production of the combined system.

### 3.2 Capacity increasing model of OFCP-P2G-GFPP

OFCP and P2G equipment are in the capacity increasing mode, as shown in Figure 4.

In order to solve the problem of time and space mismatch, carbon storage tank, liquid oxygen tank and gas storage tank are added to capacity increasing model. The total reaction stage of P2G still follows the law of conservation of mass, which can be expressed by Eq. 15 combined with the relationship between stoichiometry and the amount of substance.

$$n_c^{CH_4} - n_s^{CH_4} = n_c^{CO_2} + n_s^{CO_2} = \frac{1}{2} (n_c^{O_2} - n_s^{O_2}) = \frac{1}{4} n_c^{H_2} \quad (15)$$

In the capacity increasing operation mode of the combined system, the law of conservation of mass is used to calculate the  $CO_2$  emission.

$$\begin{aligned}
 n_{O_2}^{CO_2} &= n_i^C + n_p^{O_2} + n_c^{O_2} - n_c^{CO_2} \\
 &= n_i^C + n_p^{O_2} + \left(\frac{1}{2}n_c^{H_2} + n_s^{O_2}\right) - \left(\frac{1}{4}n_c^{H_2} - n_s^{CO_2}\right) \\
 &= n_i^C + n_p^{O_2} + \frac{1}{4}n_c^{H_2} + n_s^{O_2} + n_s^{CO_2} \\
 &= n_i^C + \frac{n_g^{O_2}}{\lambda_g^{O_2}}P_{ASU} + \frac{n_g^{CO_2}P_{CPU}}{\lambda_g^{CO_2}} + n_s^{O_2} + n_s^{CO_2}
 \end{aligned} \tag{16}$$

Due to the investment in energy storage equipment, the carbon emissions are affected by the air in and out of the oxygen storage equipment and carbon storage equipment. From the mathematical model shown in Eq. 16, we can see that it can provide a way to reduce carbon emissions.

The output electric energy  $P_{O_2}$  of the capacity increasing operation mode is solved and summed.

$$\begin{aligned}
 P_{O_2} &= P_{OFCPn2} + P_{GFPP} \\
 &= \varepsilon^{O_2} \left( n_p^{O_2} + \frac{1}{2}n_c^{H_2} + n_s^{O_2} \right) - \frac{\lambda_g^{O_2} n_p^{O_2}}{\eta_{ASU}} - \frac{\lambda_g^{CO_2} \left( \frac{1}{4}n_c^{H_2} - n_s^{CO_2} \right)}{\eta_{CPU}} \\
 &\quad + \eta_e^{CH_4} \varphi^{CH_4} \left( \frac{1}{4}n_c^{H_2} + n_s^{CH_4} + n_i^{CH_4} \right) \\
 &= \left[ \left( \varepsilon^{O_2} - \frac{\lambda_g^{O_2}}{\eta_{ASU}} \right) n_p^{O_2} - \frac{\lambda_g^{CO_2} n_c^{CO_2}}{\eta_{CPU}} \right] + \eta_e^{CH_4} \varphi^{CH_4} n_i^{CH_4} \\
 &\quad + \frac{\left( 2\varepsilon^{O_2} + \eta_e^{CH_4} \varphi^{CH_4} \right) \eta_{P2G}^{H_2}}{4\varphi^{H_2}} P_{WT} + \varepsilon^{O_2} n_s^{O_2} + \frac{\lambda_g^{CO_2} n_s^{CO_2}}{\eta_{CPU}} \\
 &\quad + \eta_e^{CH_4} \varphi^{CH_4} n_s^{CH_4} \\
 &= P_{OFCP} + \eta_e^{CH_4} E_i + \eta^e P_{WT} + P_s^{O_2} + P_s^{CO_2} + P_s^{CH_4}
 \end{aligned} \tag{17}$$

From the mathematical model shown in Eq. 17, the output power of the system increases. The input of the liquid oxygen tank provides a convenient working environment for OFCP. The input of carbon storage tanks provides clean energy raw materials for P2G equipment. The investment in gas storage tanks provides efficient operation efficiency for GFPP.

Resolve and sum the output heat of the capacity-increasing operation model  $H_{O_2}$ .

$$\begin{aligned}
 H_{O_2} &= H_{P2G} + H_{GFPP} \\
 &= \varphi_{te} \left( \frac{1}{4}n_c^{H_2} + n_s^{CH_4} \right) + \eta_h^{CH_4} \varphi^{CH_4} \left( \frac{1}{4}n_c^{H_2} + n_s^{CH_4} + n_i^{CH_4} \right) \\
 &= \eta_h^{CH_4} E_i + \eta^h P_{WT} + \left( \varphi_{te} + \eta_h^{CH_4} \varphi^{CH_4} \right) n_s^{CH_4} \\
 &= \eta_h^{CH_4} E_i + \eta^h P_{WT} + P_s^{CH_4}
 \end{aligned} \tag{18}$$

From the mathematical model shown in Eq. 18, the output heat energy of the system increases. The input of gas storage tank has a great influence on the output of the thermal system, which can improve the heating performance of the system.

## 4 Optimal operation of OFCP-P2G-GFPP regional integrated energy system

Based on the electricity-gas regional integrated energy system, the thermal power unit will be transformed into a low-carbon.

And P2G is used to realize energy circulation, thus forming OFCP-P2G-GFPP regional integrated energy system. The operation mode of the combined system is determined by each sub module. The output energy is affected by input energy, renewable energy, energy storage equipment and operation constraints of each unit. It is more necessary to analyze the operation mechanism of OFCP-P2G-GFPP combined multi-energy system.

### 4.1 Objective function

Minimize system operating costs  $F_g$  in RIES. It includes thermal power cost  $f_{cfg}$ , wind power cost  $f_{wt}$ , P2G operation cost  $f_{P2G}$ , natural gas cost  $f_{gas}$ , gas storage operation cost  $f_{gs}$  and carbon emission cost  $f_{ct}$ . During the operation of the unit, the operation cost is calculated according to the real-time output power of the unit. As shown in Eqs 19–25. In the carbon trading market, the carbon emission quota is set, and the carbon emission is strictly controlled. If the carbon emission exceeds the quota, it will be punished.

$$\min F_g = f_{cfg} + f_{wt} + f_{P2G} + f_{gas} + f_{gs} + f_{ct} \tag{19}$$

$$f_{cfg} = a_u (P_Z)^2 + b_u P_Z + c_u \tag{20}$$

$$f_{wt} = C_{wt} P_{WT} \tag{21}$$

$$f_{P2G} = \eta_{P2G}^{CH_4} C_{P2G} P_{WT} \tag{22}$$

$$f_{gas} = C_{gas} n_i^{CH_4} \tag{23}$$

$$f_{gs} = C_{gs}^{CH_4} n_s^{CH_4} + C_{gs}^{CO_2} n_s^{CO_2} + C_{gs}^{O_2} n_s^{O_2} \tag{24}$$

$$f_{ct} = C_{ct}^{CO_2} \left( n_o^{CO_2} - n_{norm}^{CO_2} \right) \tag{25}$$

In the equation:  $a_u, b_u, c_u$  respectively represent the energy consumption characteristic curve parameters of thermal power units.  $C_{wt}, C_{P2G}, C_{gas}, C_{ct}^{CO_2}$  are the cost coefficients of wind turbine, P2G, gas source and carbon market transaction respectively.  $C_{gs}^{CH_4}, C_{gs}^{CO_2}, C_{gs}^{O_2}$  are the cost coefficients of each energy storage device.  $P_Z$  represents the effective electric energy generated by the thermal power unit.  $P_{WT}$  represents the power accepted by the wind turbine;  $n_{norm}^{CO_2}$  indicates the allowable carbon allowance for thermal power units.

### 4.2 Constraint conditions

#### 4.2.1 Internal constraints of energy hubs

(1) Constraints of ASU output

$$0 \leq n_p^{O_2} \leq n_{p,max}^{O_2} \tag{26}$$

In the inequality:  $n_p^{O_2}$  represents the amount of oxygen produced by ASU in OFCP and  $n_{p,max}^{O_2}$  represents the upper limit of output.

(2) Constraints of CPU output

$$0 \leq n_c^{CO_2} \leq n_{c,max}^{CO_2} \tag{27}$$

In the inequality:  $n_c^{CO_2}$  represents the amount of CO<sub>2</sub> captured by the CPU during operation and  $n_{c,max}^{CO_2}$  represents the upper limit of output.

(3) Constraints of natural gas output

$$0 \leq n_i^{CH_4} \leq n_{i,max}^{CH_4} \tag{28}$$

In the inequality:  $n_i^{CH_4}$  represents the amount of natural gas provided by the external gas source for the gas turbine and  $n_{i,max}^{CH_4}$  represents the upper limit of output.

(4) Constraints of P2G output

$$0 \leq n_c^{CH_4} \leq n_{c,max}^{CH_4} \tag{29}$$

In the inequality:  $n_c^{CH_4}$  is the natural gas flow rate of P2G equipment, and  $n_{c,max}^{CH_4}$  is the peak output. In the same way, other gas output constraints of P2G can be obtained from Eq. 4 of the law of conservation of mass.

(5) Constraints of gas storage device

The specific expressions of the gas storage device model are the balance conditions of gas storage capacity shown in Eqs 30–32, the limit constraints of gas storage capacity shown in inequalities Eq. 33, 34, and the input and output flow constraints shown in inequalities Eqs 36, 37, 38.

$$n_s^{CH_4}(t) = S^{CH_4}(t) - S^{CH_4}(t+1) \tag{30}$$

$$n_s^{CO_2}(t) = S^{CO_2}(t) - S^{CO_2}(t+1) \tag{31}$$

$$n_s^{O_2}(t) = S^{O_2}(t) - S^{O_2}(t+1) \tag{32}$$

$$S_{min}^{CH_4} \leq S^{CH_4}(t) \leq S_{max}^{CH_4} \tag{33}$$

$$S_{min}^{CO_2} \leq S^{CO_2}(t) \leq S_{max}^{CO_2} \tag{34}$$

$$S_{min}^{O_2} \leq S^{O_2}(t) \leq S_{max}^{O_2} \tag{35}$$

$$n_{smin}^{CH_4} \leq n_s^{CH_4}(t) \leq n_{smax}^{CH_4} \tag{36}$$

$$n_{smin}^{CO_2} \leq n_s^{CO_2}(t) \leq n_{smax}^{CO_2} \tag{37}$$

$$n_{smin}^{O_2} \leq n_s^{O_2}(t) \leq n_{smax}^{O_2} \tag{38}$$

In the equation:  $S^{CH_4}(t)$ ,  $S^{CO_2}(t)$ ,  $S^{O_2}(t)$  indicate the gas storage capacity of  $CH_4$ ,  $CO_2$  and  $O_2$  gas storage units at time  $t$ . Within the time interval, the difference between two adjacent gas storage capacities is equal to the gas flow.  $S_{min}^{CH_4}$  and  $S_{max}^{CH_4}$  respectively represent the upper and lower limits of natural gas storage capacity.  $S_{min}^{CO_2}$  and  $S_{max}^{CO_2}$  respectively represent the upper and lower limits of carbon storage capacity.  $n_s^{CH_4}(t)$ ,  $n_s^{CO_2}(t)$ ,  $n_s^{O_2}(t)$  indicate the gas flow of each energy storage device at time  $t$ .  $n_{smax}^{CH_4}$ ,  $n_{smax}^{CO_2}$ ,  $n_{smax}^{O_2}$  respectively represent the peak value of each gas flow rate.

After the system runs in a scheduling period, the total in and out of energy storage equipment is not counted. Restore it to the initial value to leave enough adjustment space for the next cycle:

$$\sum_{t=1}^T n_s(t) = 0 \tag{39}$$

### 4.2.2 Load balancing constraints

In the constructed OFCP-P2G-GFPP regional integrated energy system, the node power balance conditions are shown in Eq. 40, and the constraint conditions of P2G wind curtailment are shown in Eq. 41 and 42.

$$L_m(t) = P_{o1}(t) + W_e(t) \tag{40}$$

$$W_f(t) = W_e(t) + W_d(t) + P_{WT}(t) \tag{41}$$

$$P_{wt,min} \leq P_{wt}(t) \leq P_{wt,max} \tag{42}$$

In the equation:  $L_m(t)$  represents the electric load during  $t$  period,  $P_{o1}(t)$  is the output energy of thermal power unit at time  $t$ ,  $P_{wt}(t)$  is the abandoned wind consumption of P2G using wind turbines at time  $t$ ,  $W_e(t)$  is the renewable energy available at time  $t$ ,  $W_f(t)$  is the wind turbine power transmission at time  $t$ ,  $W_d(t)$  is the abandoned air volume of wind turbine at time  $t$ ,  $P_{wt,min}$  and  $P_{wt,max}$  respectively represent the upper and lower limits of P2G to eliminate wind.

### 4.2.3 System constraints of OFCP-P2G-GFPP

The OFCP-P2G-GFPP system first needs to meet the power output constraints. On the one hand, the power output constraint is affected by the output of thermal power units and gas turbines, and there are upper and lower limits for the output power of the units, as shown in inequalities (43) and (44). On the other hand, it is restricted by the consumption of renewable energy, as shown in inequality (45).

$$P_o(t) \leq P_{zmax} + P_{emax} - \frac{\lambda_g^{CO_2, H_2} \eta_{P2G}}{4\eta_{CPU}^{CO_2, H_2}} P_{WT}(t) - \frac{\lambda_g^{O_2}}{\eta_{ASU}} n_p^{O_2}(t) \tag{43}$$

$$P_o(t) \geq P_{zmin} + P_{emin} - \frac{\lambda_g^{CO_2, H_2} \eta_{P2G}}{4\eta_{CPU}^{CO_2, H_2}} P_{WT}(t) - \frac{\lambda_g^{O_2}}{\eta_{ASU}} n_p^{O_2}(t) \tag{44}$$

$$\begin{cases} P_o(t) \geq P_{OFCP}(t) + \eta_e^{CH_4} E_1(t) + \eta^e P_{WTmin}(t) \\ P_o(t) \leq P_{OFCP}(t) + \eta_e^{CH_4} E_1(t) + \eta^e P_{WTmax}(t) \end{cases} \tag{45}$$

Combining the output constraints under two different conditions, the operating range of the system is shown in Figure 5. Natural gas source provides energy for independent operation of gas turbine, and the output of the system is a linear curve passing through the origin. When the same natural gas energy is input, with the integration of OFCP and the consumption of renewable energy, the system operation curve gradually tends to be highly efficient. Under the system constraints, the power output range of the system increases, and the system operates flexibly within this range.

In addition, the OFCP-P2G-GFPP system also needs to meet the thermal power output constraints. Since the output power of the gas turbine has upper and lower limits, the output range of the gas turbine affects the thermal power output of the system, as shown in inequality (46). Secondly, the thermal power output of the system is

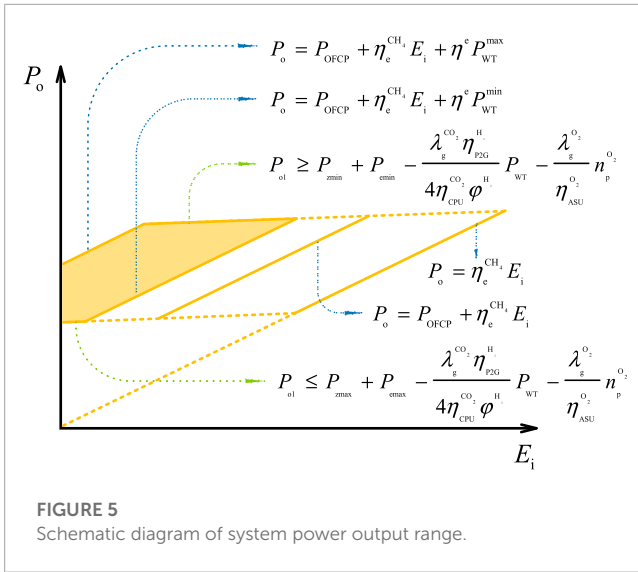


FIGURE 5 Schematic diagram of system power output range.

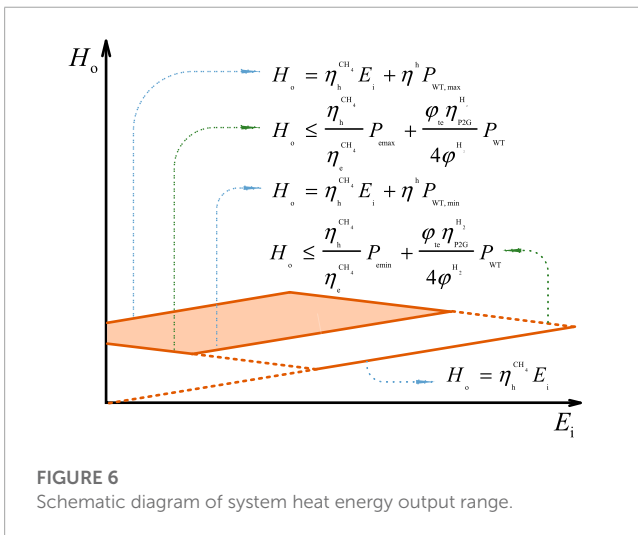


FIGURE 6 Schematic diagram of system heat energy output range.

also affected by the consumption of renewable energy, as shown in inequality (47).

$$\begin{cases} H_o(t) \geq \frac{\eta_h^{CH_4}}{\eta_e^{CH_4}} P_{emin} + \frac{\varphi_{te}^{H_2} \eta_{P2G}^{H_2}}{4\varphi^{H_2}} P_{WT}(t) \\ H_o(t) \leq \frac{\eta_h^{CH_4}}{\eta_e^{CH_4}} P_{emax} + \frac{\varphi_{te}^{H_2} \eta_{P2G}^{H_2}}{4\varphi^{H_2}} P_{WT}(t) \end{cases} \quad (46)$$

$$\begin{cases} H_o(t) \geq \eta_h^{CH_4} E_i(t) + \eta^h P_{WTmin}(t) \\ H_o(t) \leq \eta_h^{CH_4} E_i(t) + \eta^h P_{WTmax}(t) \end{cases} \quad (47)$$

The operating range of system thermal power can be obtained from the output constraint in the same way, as shown in Figure 6. The system inputs the same natural gas energy, and compared with the independent operation of the gas turbine, the range of the OFCP-P2G-GFPP system's output heat energy is increased, and the flexibility of operation is improved.

### 4.3 Establish a low-carbon economic model

#### 4.3.1 Assumptions

Since the main concern is the carbon emission and wind curtailment of RIES, it is assumed that the gases are in standard temperature and pressure. If there are other gases state in actual operation, corresponding constraints can be added to the model. In order to simplify the dispatching model, only the combination of OFCP-P2G-GFPP system and renewable energy is considered, and other types of generating units are ignored. If there are other types of units in the actual scheduling, the corresponding constraints can be added to the model. In order to linearize the processing system, the minimum input power of unit equipment is ignored. Start stop constraints can be added in actual scheduling. The objective function is the optimal economic cost. Other objective functions can also be applied to this study. This will not affect the system of OFCP-P2G-GFPP.

#### 4.3.2 Separate operation mode of OFCP and GFPP

There are no coupling components such as P2G devices in the discrete operation mode. There are no energy transmission and conversion between units, and they all operate independently. The dispatching model is shown in the following equation.

$$\begin{cases} L_m(t) = P_{o1}(t) + W_e(t) \\ P_{o1}(t) = P_{OFCP}(t) + \eta_e^{CH_4} E_i(t) \\ H_{o1}(t) = \eta_h^{CH_4} E_i(t) \end{cases} \quad (48)$$

#### 4.3.3 Basic operating mode of OFCP-P2G-GFPP

OFCP-P2G-GFPP direct energy transmission and conversion between units. At the same time, the conversion time shift is ignored, that is, the CO<sub>2</sub> emitted by the OFCP is instantly converted into CH<sub>4</sub> under the action of P2G. The energy flow parameters used in the basic operation model are shown in Figure 2, and the scheduling model is shown in the following equation.

$$\begin{cases} L_m(t) = P_{o1}(t) + W_e(t) \\ P_{o1}(t) = P_{OFCP}(t) + \eta_e^{CH_4} E_i(t) + \eta^e P_{WT}(t) \\ H_{o1}(t) = \eta_h^{CH_4} E_i(t) + \eta^h P_{WT}(t) \end{cases} \quad (49)$$

#### 4.3.4 Capacity increasing operation mode of OFCP-P2G-GFPP

In order to solve the problem of inequality between time and space, the capacity-increasing model adds storage equipment to the premise of the basic model. The scheduling model is shown in the following equation.

$$\begin{cases} L_m(t) = P_{o2}(t) + W_e(t) \\ P_{o2}(t) = P_{OFCP}(t) + \eta_e^{CH_4} E_i(t) + \eta^e P_{WT}(t) \\ \quad + \left[ \varepsilon^{O_2} n_s^{O_2}(t) + \frac{\lambda_g^{CO_2}}{\eta_{CPU}^{CO_2}} n_s^{CO_2}(t) + \eta_e^{CH_4} \varphi^{CH_4} n_s^{CH_4}(t) \right] \\ H_{o2}(t) = \eta_h^{CH_4} E_i(t) + \eta^h P_{WT}(t) + (\varphi_{te} + \eta_h^{CH_4} \varphi^{CH_4}) n_s^{CH_4}(t) \end{cases} \quad (50)$$

## 5 Example analysis

In this section, according to the different operating modes of the system, three cases are set, and then comparative analysis is carried out. Taking the economic cost of system operation as the optimal objective, the impact of carbon dioxide emissions and renewable energy acceptance capacity on the system is analyzed. Compare the separate operating units with the OFCP-P2G-GFPP combined system, and analyze the changes in the output of thermal power units and external natural gas. After comparing the differences between the basic mode and the capacity increasing mode of OFCP-P2G-GFPP combined system, the impacts of the system on CO2 emissions and renewable energy utilization are analyzed. Firstly, referring to the typical daily load in winter in reference (Yang, 2019), the typical parameters of facilities in OFCP-P2G-GFPP combined system are determined, and the scheduling period is 24 h. Secondly, the IPOPT solver based on the interior point method in the optimization software GAMS is used to optimize the solution.

### 5.1 Typical parameters

There are many parameters in the model of OFCP-P2G-GFPP combined system. Typical values of carbon capture technology and oxy-fuel combustion technology are shown in literature (Cui et al., 2020)- (Chen et al., 2010). In the transformation process of P2G technology, the required physical quantities are shown in literature (Hoekman et al., 2010). and the constraints of each unit are shown in literature (Yang, 2019). In order to unify the parameter unit, according to the gas molar volume equation and the ideal gas equation of state, the parameter values are converted to standard values. Typical operation parameters of each unit are shown in Table 1.

The common cost coefficients of thermal power units, natural gas sources and wind turbines are shown in literature (Jiang, 2018) and (Zeng et al., 2016), P2G operating cost coefficient is shown in literature (Guandalini et al., 2015), and the cost of energy storage equipment is shown in literature (Yang, 2019), (Touretzky et al., 2016) and (Wang et al., 2014). Same as above, the parameter values need to be converted uniformly. The typical cost coefficients are shown in Table 2.

TABLE 1 Typical parameters of the system.

Description	Value
Energy consumption per unit CO <sub>2</sub> capture	$\lambda_g^{CO_2} = 8.8 \times 10^{-6} \text{MWh/mol}$
CO <sub>2</sub> capture efficiency	$\eta_{CP}^{CO_2} = 90\%$
Energy consumption per unit of oxygen	$\lambda_g^{O_2} = 6.79 \times 10^{-6} \text{MWh/mol}$
Oxygen production efficiency	$\eta_{ASU}^{O_2} = 95\%$
Heat energy per unit methane reaction	$\varphi_{te} = 4.6 \times 10^{-5} \text{MWh/mol}$
Calorific value of natural gas	$\varphi^{H_2} = 6.7 \times 10^{-5} \text{MWh/mol}$
Energy conversion efficiency of P2G	$\eta_{P2G}^{H_2} = 50\%$
Electric conversion efficiency of GFPP	$\eta_e^{CH_4} = 60\%$
Heat conversion efficiency of GFPP	$\eta_h^{CH_4} = 20\%$

The typical daily load curve and the predicted output curve of wind farm in literature (Yang, 2019) are partially modified, as shown in Figure 7.

In order to study the characteristic relationship of OFCP-P2G-GFPP combined system, the objective function is to optimize the economic cost of operation. According to the difference of the introduction of P2G, this article sets the following three cases for comparative analysis.

Case 1 Ignore P2G technology, OFCP and GFPP run independently.

Case 2 Considering P2G technology, power-to-gas technology combines OFCP with gas turbines, which constitutes the basic scheduling model for the joint operation of OFCP-P2G-GFPP system.

Case 3 Considering P2G technology, on the premise of basic scheduling model of OFCP-P2G-GFPP system, add energy storage equipment with multiple gases. Then the capacity increase scheduling model of OFCP-P2G-GFPP system is constructed.

### 5.2 Comparative analysis of different scheduling schemes

This article considers the operation of the system in the above three cases and analyzes the advantages of the OFCP-P2G-GFPP combined system. The specific costs are shown in Table 3.

TABLE 2 Typical cost coefficients.

Description	Value
Energy consumption parameters	$a_u = 0.0024, b_u = 12.33, c_u = 28$
Wind turbine cost coefficients	$C_{wt} = 8\$/\text{MWh}$
P2G cost coefficients	$C_{P2G} = 18\$/\text{MWh}$
Natural gas source cost coefficients	$C_{gas} = 1.904 \times 10^{-3}\$/\text{mol}$
Carbon trading cost coefficient	$C_{ct}^{CO_2} = 6.286 \times 10^{-4}\$/\text{mol}$
Cost coefficients of natural gas storage equipment	$C_{gs}^{CH_4} = 4.413 \times 10^{-4}\$/\text{mol}$
Cost coefficients of carbon storage equipment	$C_{gs}^{CO_2} = 3.151 \times 10^{-4}\$/\text{mol}$
Cost coefficients of oxygen storage equipment	$C_{gs} = 1.904 \times 10^{-3}\$/\text{mol}$

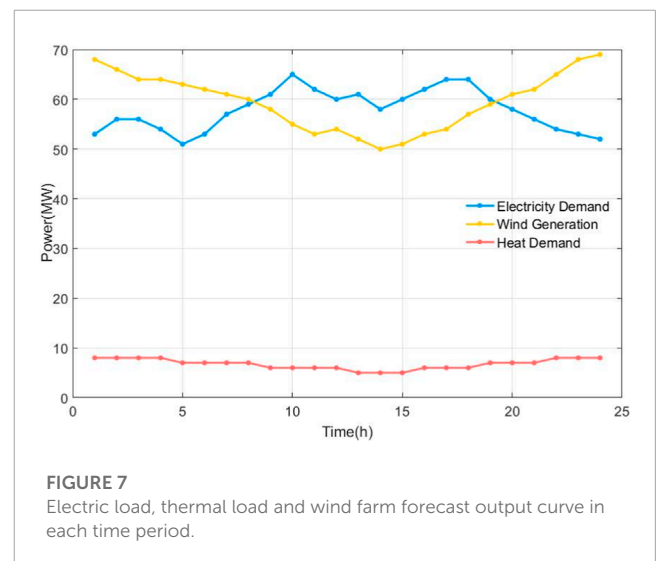


FIGURE 7 Electric load, thermal load and wind farm forecast output curve in each time period.

**TABLE 3** System operating cost table.

Cost	Case1	Case2	Case3
OFCP/\$	4,644	4,048	2,469
Natural gas fuel/\$	4,559	2,870	1,148
Wind abandonment/\$	4,853	1,352	172
CO <sub>2</sub> emission/\$	7,719	5,756	3,388
P2G operation/\$	-	5,759	7,086
Energy storage equipment/\$	-	-	4,525
Total/\$	21,778	19,786	18,791

Case 2 saves 1991\$ in total cost compared with Case 1, which is 9.14%. The cost of carbon emission is significantly reduced, and the carbon dioxide emission is effectively improved. Case 3 saves 2986\$ in total cost compared with Case 1, which is 13.05%. The cost of abandoned wind is greatly reduced, and the absorption effect and flexible operation ability of abandoned wind are effectively improved. It is proved that the joint operation of OFCP-P2G-GFPP system is effective in low-carbon economic dispatch. Case 3 saves 995\$ in total cost compared to Case 2. In order to absorb more abandoned wind, the output of P2G is increased, but the energy storage equipment improves the energy utilization rate, the system operation cost is reduced. The unit output of Case 1, as shown in Figure 8.

As can be seen from the above figure, in Case 1, OFCP, gas turbine, and wind power operate independently to supply electricity load. Natural gas fuel acts on the gas turbine, and the heat energy produced is used to meet the demand for heat load. Separate operation of each unit causes unnecessary energy waste and high costs. The unit output of electric load in Case 2 and Case 3, as shown in Figure 8.

In the joint operation mode of OFCP-P2G-GFPP, OFCP, gas turbine, P2G equipment and wind turbine are coordinated and optimized. Compared with Case 1, Case 2 can make rational use of renewable energy and effectively improve the wind curtailment capacity of the system. In the capacity increasing operation mode of OFCP-P2G-GFPP system, Case 3 consumes more abandoned wind than Case 2. Considering the daily balance of the energy storage equipment, the energy storage equipment increases the net load when the electric load is low, and releases the stored energy when the electric load is high. And through the coordination of energy storage equipment, the mode of electricity determined by gas is broken. The OFCP-P2G-GFPP combined system closely couples electricity, gas, and thermal energy systems to achieve complementary advantages among regional integrated energy systems.

In conclusion, the optimal wind power accommodation and economic operation can be achieved through the coordination of RIES.

The output of OFCP excluding wind power accommodation is in three cases. The output of OFCP considering wind power accommodation is in three cases, as shown in Figure 9.

Only the internal output of the OFCP unit is considered, and the additional issuance of renewable energy consumption is ignored.

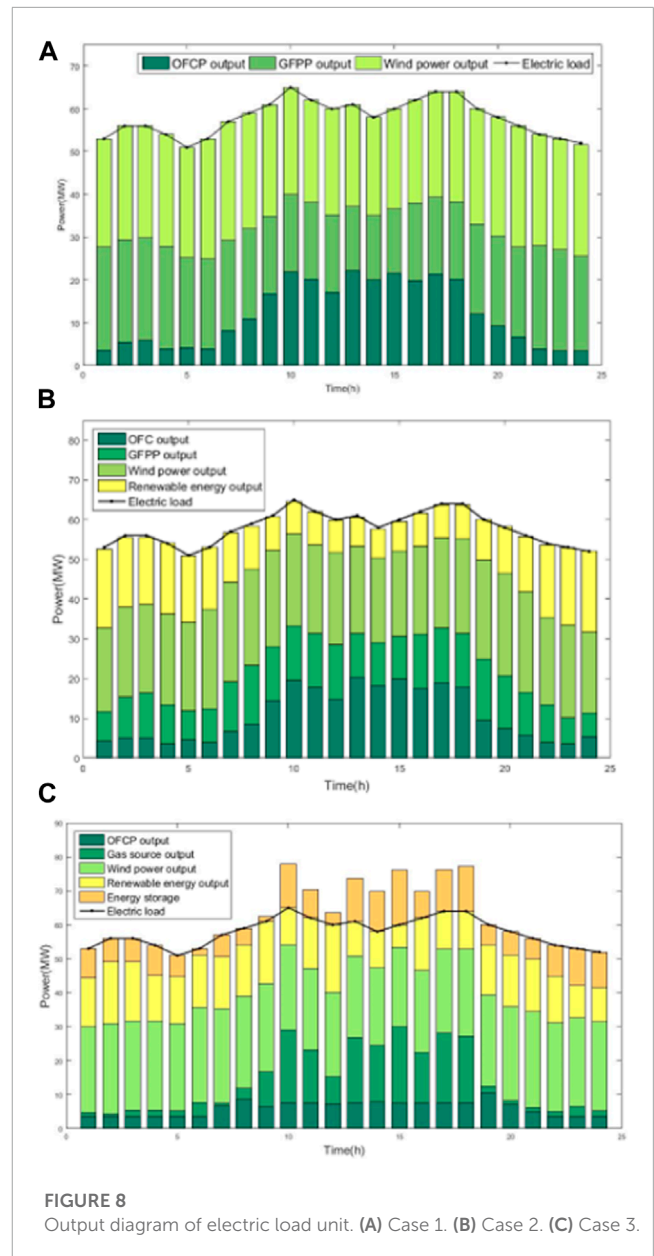
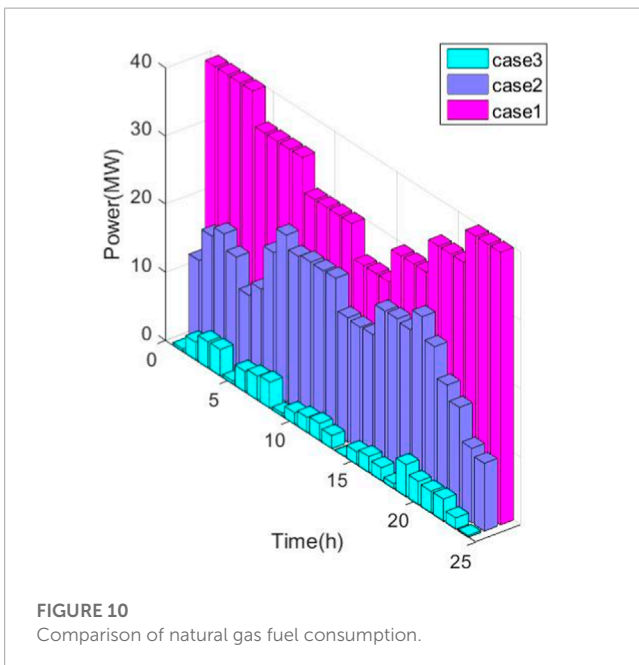
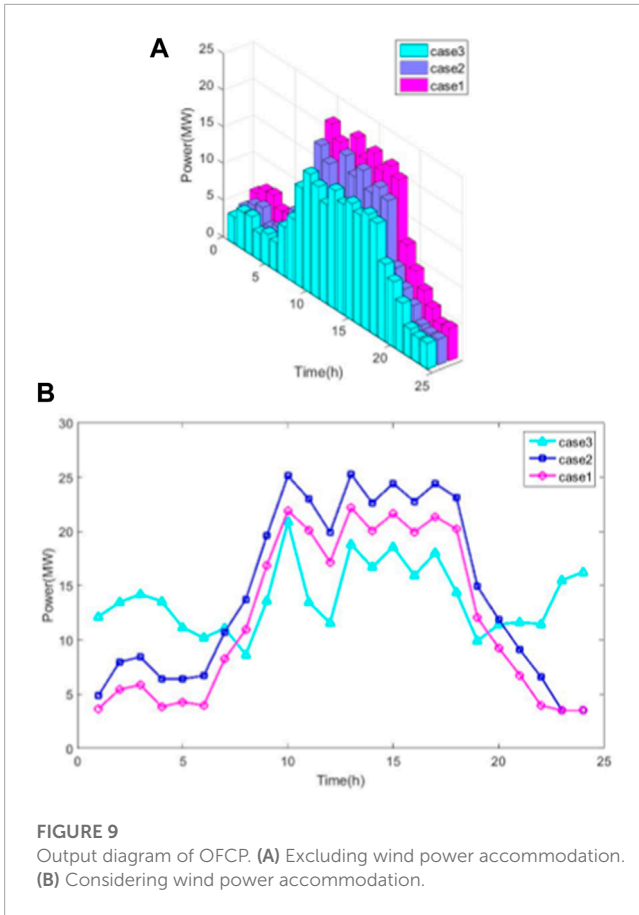


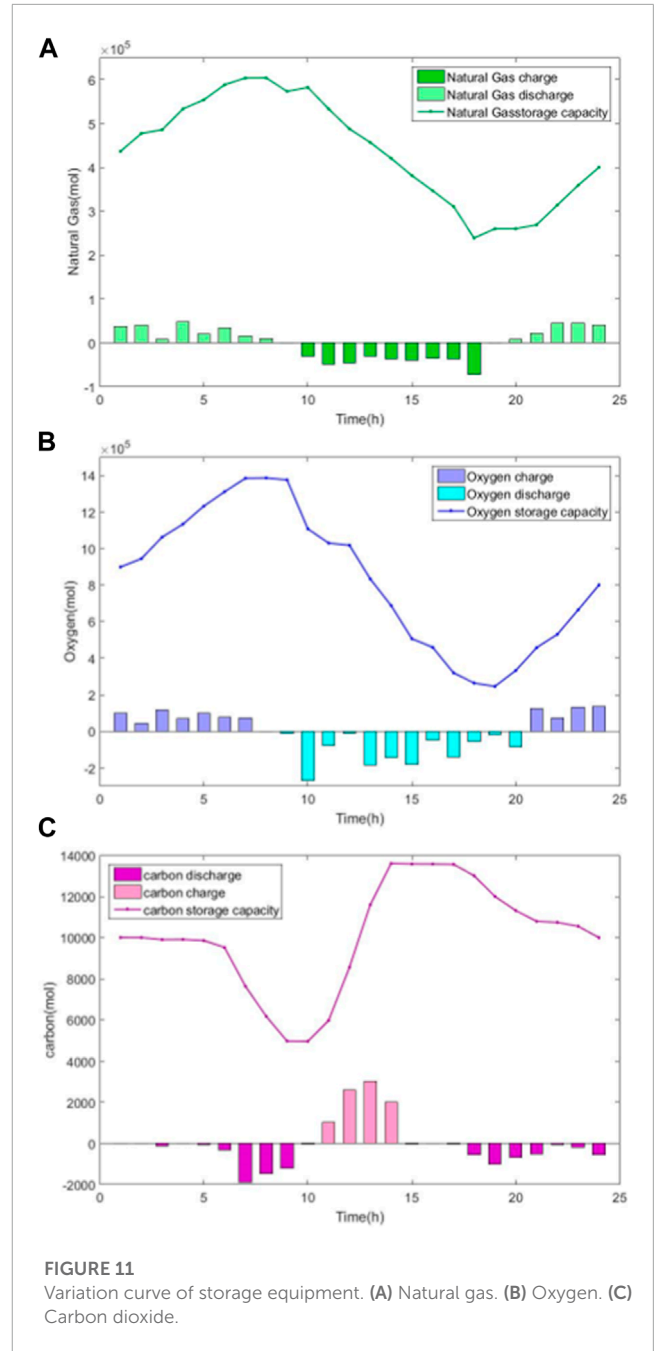
**FIGURE 8** Output diagram of electric load unit. (A) Case 1. (B) Case 2. (C) Case 3.

It can be seen from Figure 9 that the power output of Cases 2 and 3 is reduced compared to Case 1. The OFCP-P2G-GFPP combined system can effectively alleviate the power supply pressure of thermal power units, reduce the amount of oxygen produced by ASU, and reduce the loss generated during the operation of the unit.

The energy generated by wind power accommodation is included in the output of the OFCP. It can be seen from Figure 9 that the output of Case 2 is increased compared to Case 1. The OFCP-P2G-GFPP combined system improves the capacity of abandoning wind and when the electricity consumption peaks, which converts the renewable energy into other forms of energy to meet the electricity demand. In Case 3, additional energy storage equipment is added to give it an advantage in peak load shifting. During the period of low power generation from 1 to 7 o'clock and 20 to

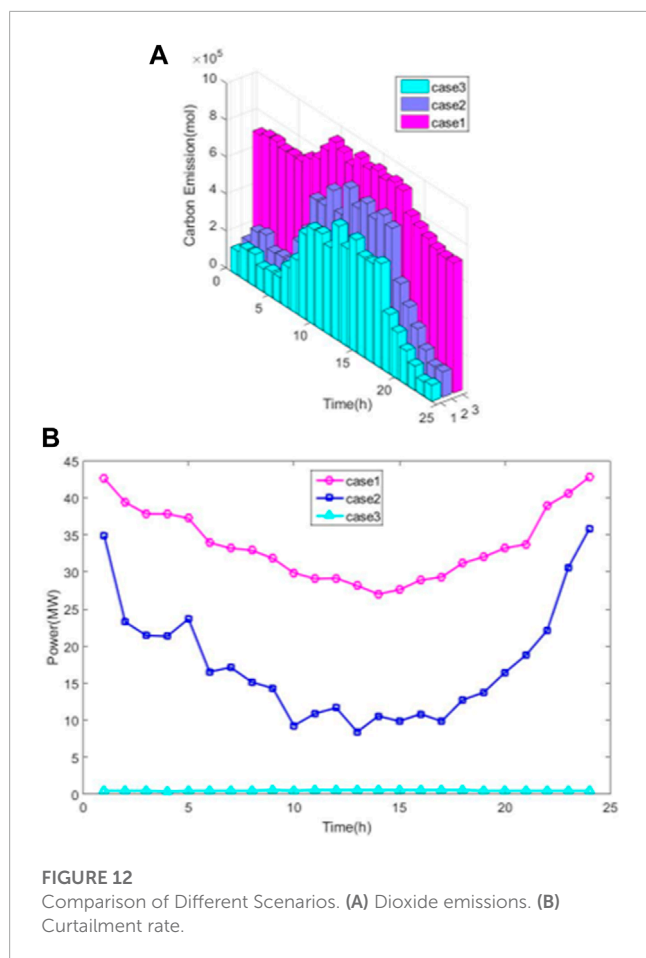


24 o'clock, the power output of Case 3 is greater than that of Case 2. However, during the period of 8–19 ignition electricity generation, the power output of Case 3 is less than Case 2. The reason lies in the coordination of OFCP and oxygen storage equipment, GFPP and gas storage equipment. When the load is low, OFCP



and GFPP consume more energy to generate O<sub>2</sub> and CH<sub>4</sub> and inject them into the gas storage equipment. When the load is peak, the unit no longer needs to consume too much energy, and uses the stored gas for energy supply, which realizes the load transfer. The use of natural gas fuel in three cases, as shown in Figure 10.

From Figure 10, it can be seen that Cases 2 and 3 have reduced natural gas fuel usage compared to Case 1. The main reason is that in Cases 2 and 3, the remaining wind power will be reused, and GFPP will obtain additional CH<sub>4</sub> from P2G, to reduce the use of purchased natural gas and save the cost of raw materials. The joint operation of OFCP-P2G-GFPP provides a new solution to the problem of renewable energy acceptance. Case 3 utilizes the



space-time translation characteristics of energy storage equipment to further increase the ability wind power accommodation. The change curves of three types of energy storage equipment, as shown in Figure 11.

Due to the anti-peaking characteristics of wind power, during the low period of electric load, wind power output is in the peak period. OFCP-P2G-GFPP combined system capacity expansion mode use two reaction stages of P2G technology. Carbon storage is consumed, and a large amount of abandoned wind is converted into O<sub>2</sub> and CH<sub>4</sub> for storage, which improves the system's ability to absorb renewable energy. And it effectively increases the net load, and plays the role of "filling valley". During the peak period of electricity load, wind power output is at a trough period. The stored gas will be supplied to OFCP and GFPP and the captured CO<sub>2</sub> will be stored to increase the output to reduce the net load and play the role of "peak shaving". In this way, through the coordination of coupling elements and energy storage equipment, the effect of load transfer can be achieved, and the goal of carbon dioxide emission reduction can be achieved. The comparison of CO<sub>2</sub> emission and wind abandonment rate under three cases, as shown in Figure 12.

The CO<sub>2</sub> captured by CPU can be used for P2G to reduce CO<sub>2</sub> emissions by absorbing renewable energy. It can be seen from Figure 12 that OFCP-P2G-GFPP combined system has good characteristics of low-carbon emission reduction and wind

curtailment. After adding the energy storage equipment, the carbon emission and wind abandonment rate are significantly reduced.

## 6 Conclusion

Firstly, the OFCP-P2G-GFPPP composite system was proposed to analyze the relationship between energy flows within the system. Secondly, in the regional comprehensive energy system, establish an optimized scheduling model for the operation of the OFCP-P2G-GFPPP system. Finally, analyze the operating characteristics of two different modes. The characteristics and advantages of its basic model and capacity expansion model were discussed respectively, in order to improve the flexible operation mode of the comprehensive energy system.

- (1) The OFCP-P2G-GFPPP combined system can effectively alleviate the power supply pressure of thermal power units. Reduce the use of purchased natural gas and increase the consumption of renewable energy. After adding energy storage equipment, it has the ability to "cut peak and fill valley", which can achieve load transfer. OFCP-P2G-GFPPP has good low-carbon emission reduction capabilities and operational economic benefits.
- (2) According to the example, it can be concluded that compared with the independent operation model, the basic model of the OFCP-P2G-GFPPP system saves 9.14% of the total cost and reduces carbon emissions by 44.05%, which proves the importance of the OFCP-P2G-GFPPP interconnected system in the low-carbon economic dispatch of the integrated energy system.
- (3) According to the example, it can be concluded that compared with the independent operation model, the OFCP-P2G-GFPPP system expansion model saves 13.05% of the total cost and reduces carbon emissions by 59.91%. Compared with the basic model, the OFCP-P2G-GFPPP system expansion model saves 4.82% of the total cost and reduces carbon emissions by 28.34%. It proves the rationality of considering energy storage equipment and OFCP-P2G-GFPPP interconnection system in the low-carbon economic dispatch of the integrated energy system.

## Data availability statement

The original contributions presented in the study are included in the article/supplementary material, further inquiries can be directed to the corresponding author.

## Author contributions

RW: Supervision, Formal analysis, Writing–review and editing; XW: Writing-Original draft preparation; Formal analysis, Validation, Supervision, XW: Writing–review and editing, Validation; YF: Writing–review and editing, Validation; YZ: Supervision. All authors contributed to the article and approved the submitted version.

## Funding

This work was supported by the Project of Jilin Province Education Department (JJKH20230118KJ).

## Conflict of interest

YZ was employed by the State Grid Jibei Electric Power Company, Chengde Power Supply Company.

The remaining authors declare that the research was conducted in the absence of any commercial or financial

relationships that could be construed as a potential conflict of interest.

## Publisher's note

All claims expressed in this article are solely those of the authors and do not necessarily represent those of their affiliated organizations, or those of the publisher, the editors and the reviewers. Any product that may be evaluated in this article, or claim that may be made by its manufacturer, is not guaranteed or endorsed by the publisher.

## References

- Chen, Q., Kang, C., and Xia, Q. (2010). Modeling flexible operation mechanism of CO<sub>2</sub> capture power plant and its effects on power-system operation. *IEEE Trans. Energy Convers.* 3 (25), 853–861. doi:10.1109/tec.2010.2051948
- Cui, Y., Zeng, P., and Zhong, W. (2020). Low-carbon economic dispatch of electricity-heat integrated energy system considering oxy-fuel combustion technology. *Proc. CSEE* 40 (18), 5827–5837. doi:10.13334/j.0258-8013.pcsee.191708
- Dong, C., and Zhao, J. (2014). From smart grid to energy Internet: Basic concepts and research framework. *Automation Electr. Power Syst.* 38 (15), 1–11. doi:10.7500/AEPS20140613007
- Energy Resource Guide (2010). Germany invented "electricity to gas" method to solve the problem of renewable energy storage. *Pet. Eng. Constr.* 3, 108–109.
- Favre-Perrod, P. (2005). "A vision of future energy networks," in 2005 IEEE power engineering society inaugural conference and exposition in Africa, Durban, South Africa, 11–15 July 2005 (IEEE), 13–17.
- Geidl, M. (2007). *Integrated modeling and optimization of multi-carrier energy system*. Zurich: ETH, 16.
- Ghorbani, B., Mehrpooya, M., and Ghasemzadeh, H. (2018). Investigation of a hybrid water desalination, oxy-fuel power generation and CO<sub>2</sub> liquefaction process. *Energy* 1 (158), 1105–1119. doi:10.1016/j.energy.2018.06.099
- Gu, W., Wang, J., Lu, S., Luo, Z., and Wu, C. (2017). Optimal operation for integrated energy system considering thermal inertia of district heating network and buildings. *Appl. Energy* 199, 234–246. doi:10.1016/j.apenergy.2017.05.004
- Guandalini, G., Campanari, S., and Romano, M. C. (2015). Power-to-gas plants, and gas turbines for improved wind energy dispatch ability: Energy and economic assessment. *Appl. Energy* 1 (147), 117–130. doi:10.1016/j.apenergy.2015.02.055
- Hoekman, S. K., Broch, A., Robbins, C., and Purcell, R. (2010). CO<sub>2</sub> recycling by reaction with renewably-generated hydrogen. *Greenh. Gas. Control* 1 (4), 44–50. doi:10.1016/j.ijggc.2009.09.012
- Hua, W., Jiang, J., and Suna, H. (2020). A blockchain based peer-to-peer trading framework integrating energy and carbon markets. *Appl. Energy* 279, 115539. doi:10.1016/j.apenergy.2020.115539
- Jiang, T. (2018). Optimal energy flow and nodal energy pricing in carbon emission-embedded integrated energy systems. *CSEE J. Power Energy Syst.* 2 (4), 179–187. doi:10.17775/cseejpes.2018.00030
- Karjunen, H., Tynjälä, T., and Hyppänen, T. (2017). A method for assessing infrastructure for CO<sub>2</sub> utilization: A case study of Finland. *Appl. Energy* 205, 33–43. doi:10.1016/j.apenergy.2017.07.111
- Lu, P., Ye, L., and Tang, Y. (2019). Research on multi-time scale active power optimal dispatching strategy of wind power cluster based on model predictive control. *Proc. CSEE* 39 (22), 6572–6583. doi:10.13334/j.0258-8013.pcsee.190188
- Touretzky, C. R., McGuffin, D. L., Ziesmer, J. C., and Baldea, M. (2016). The effect of distributed electricity generation using natural gas on the electric and natural gas grids. *Appl. Energy Sep.* 177, 500–514. doi:10.1016/j.apenergy.2016.05.098
- UNCC (2016). *Paris climate change agreement-climate change agreement*. Paris: United Nation Climate Change.
- Viebahn, P., Vallentin, D., and Höller, S. (2015). Prospects of carbon capture and storage (CCS) in India's power sector – An integrated assessment. *Appl. Energy* 157, 229–244. doi:10.1016/j.apenergy.2015.07.023
- Viebahn, P., Vallentin, D., and Höller, S. (2014). Prospects of carbon capture and storage (CCS) in China's power sector – An integrated assessment. *Appl. Energy* 117, 62–75. doi:10.1016/j.apenergy.2013.11.054
- Viklund, S. B., and Karlsson, M. (2015). Industrial excess heat use: Systems analysis and CO<sub>2</sub> emissions reduction. *Appl. Energy* 152, 189–197. doi:10.1016/j.apenergy.2014.12.023
- Wang, W., Wang, D., and Jia, H. (2017). Steady-state analysis of electric power-natural gas regional integrated energy system considering the state of natural gas network. *Proc. CSEE* 37 (5), 1293–1305. doi:10.13334/j.0258-8013.pcsee.160250
- Wang, Y., Qiu, J., and Tao, Y. (2020). Low-carbon oriented optimal energy dispatch in coupled natural gas and electricity systems. *Appl. Energy* 280, 115948. doi:10.1016/j.apenergy.2020.115948
- Wang, Y., Wang, Y., Huang, Y., Yang, J., Ma, Y., Yu, H., et al. (2019). Operation optimization of regional integrated energy system based on the modeling of electricity-thermal-natural gas network. *Appl. Energy* 251, 113410. doi:10.1016/j.apenergy.2019.113410
- Wang, Z., Kuang, J. C., Pang, H. Q., and Huo, Z. L. (2014). Cost analysis of CO<sub>2</sub> geological storage in deep saline formation. *A Sci. A Technol. Rev.* 1 (31), 46–53. doi:10.3981/j.issn.1000-7857.2014.006
- Yang, J. (2019). Modeling the operation mechanism of combined P2G and gas-fired plant with CO<sub>2</sub> recycling. *IEEE Trans. Smart Grid* 1 (10), 1111–1121. doi:10.1109/tsg.2018.2849619
- Zeng, Q., Fang, J., and Li, J. (2016). Steady-state analysis of the integrated natural gas and electric power system with bi-directional energy conversion. *Appl. Energy* 184, 1483–1492. doi:10.1016/j.apenergy.2016.05.060
- Zhang, X. (2015). Optimal expansion planning of energy hub with multiple energy infrastructures. *IEEE Trans. Smart Grid* 5 (6), 2302–2311. doi:10.1109/tsg.2015.2390640
- Zhou, R., Xiao, J., and Tang, X. (2018). Coordination and optimization of electricity-to-gas consumption of new energy and carbon utilization of carbon capture power plants. *Power Autom. Equip.* 38 (7), 61–67. doi:10.16081/j.issn.1006-6047.2018.07.008